J. Biochem. **133**, 123–131 (2003)
DOI: 10.1093/jb/mvg007

Expression of a Synthetic Gene Coding for Ostrich Egg-White Lysozyme in *Pichia Pastoris* and Its Enzymatic Activity

Shunsuke Kawamura*[,1], Tamo Fukamizo[2], Tomohiro Araki[1] and Takao Torikata[1]

[1]*Department of Bioscience, School of Agriculture, Kyushu Tokai University, Aso, Kumamoto 869-1404; and* [2]*Laboratory of Enzyme System Science, Department of Food and Nutrition, Kinki University, Nakamachi, Nara 631-8505*

Received August 28, 2002; accepted November 2, 2002

To investigate the structure-function relationships of goose-type lysozyme, a gene coding for ostrich egg-white lysozyme (OEL) was designed based on the published amino acid sequence and constructed by assembling 32 chemically synthesized oligonucleotides. To obtain the recombinant OEL (rOEL), the synthetic gene was fused to the α-factor signal peptide in the expression vector pPIC9K and expressed in the methylotrophic yeast *Pichia pastoris*. The secreted protein from the transformed yeast was found to be processed at three different sites, including the correct site. The correctly processed rOEL was purified to homogeneity and shown to be indistinguishable from the authentic form in terms of circular dichroism (CD) spectrum and enzyme activity. Furthermore, the time-course of the reaction catalyzed by OEL was studied using $(GlcNAc)_n$ (n = 5 and 6) as the substrate and compared to that of goose egg-white lysozyme (GEL) [Honda and Fukamizo (1998) *Biochim. Biophys. Acta* 1388, 53–65]. OEL hydrolyzed $(GlcNAc)_6$ in an endo-splitting manner producing mainly $(GlcNAc)_2$, $(GlcNAc)_3$, and $(GlcNAc)_4$, and cleavage to $(GlcNAc)_3$ + $(GlcNAc)_3$ predominated over that to $(GlcNAc)_2$ + $(GlcNAc)_4$. This indicates that OEL hydrolyzes preferentially the third glycosidic linkage from the nonreducing end of $(GlcNAc)_6$ as in the case of GEL. The cleavage pattern seen for $(GlcNAc)_5$ was similar to that seen for $(GlcNAc)_6$. Theoretical analysis of the reaction time-course for OEL revealed that the binding free energy values for subsites B, E, and G were different between OEL and GEL, although these lysozymes were estimated to have the same type of subsite structure.

Key words: binding subsites, expression, goose-type lysozyme, ostrich, synthetic gene.

Abbreviations: OEL, ostrich egg-white lysozyme; GEL, goose egg-white lysozyme; GlcNAc, *N*-acetylglucosamine; $(GlcNAc)_n$, β-1,4-linked oligosaccharide of GlcNAc; rOEL, recombinant OEL; CD, circular dichroism; RP-HPLC, reversed-phase high performance liquid chromatography; BMGY, buffered glycerol-complex medium; BMMY, buffered methanol-complex medium; MD, minimal dextrose medium; YPD-G418, yeast extract peptone dextrose medium containing Geneticin 418.

Lysozyme, one of the best characterized carbohydrolases, cleaves the glycosidic linkage between *N*-acetylglucosamine (GlcNAc) and *N*-acetylmuramic acid in bacterial cell walls. This enzyme is classified into three types, chicken type (C-type) (*1–3*), phage type (T4-type) (*4*, *5*), and goose type (G-type) (*6–8*), based on the similarity of amino acid sequences. These three different classes of lysozymes have overall similarities in tertiary structure (*7*, *9*), although their amino acid sequences are almost entirely different. The active sites of these enzymes have a highly conserved Glu residue, which is believed to act as a general acid in catalysis (Glu35 in C-type lysozyme, Glu11 in T4-type lysozyme, Glu73 in G-type lysozyme) (*3*, *7*, *9–11*). On the other hand, the additional carboxylate ion of an Asp residue shows variability among the molecules: G-type lysozyme has no apparent counterpart to either Asp52 in C-type lysozyme or Asp20 in T4-type lysozyme (*11*). However, as yet, a definitive confirmation of the precise role of the second acidic residue in catalysis has not been obtained.

G-type lysozyme also differs from the C-type in that it is much more specific for peptide-substituted substrates (*12*). C-type lysozyme hydrolyzes a homopolymer (chitin) effectively, while G-type lysozyme is a poor catalyst of the hydrolysis of this substrate. The differences in the substrate specificity between these lysozymes are not well understood.

Much information on the structural properties and enzymatic mechanisms of C-type and T4-type lysozymes has been accumulated thus far. Relative to the considerable knowledge of these lysozymes, however, information on G-type lysozyme is quite limited. The primary structure has been reported for only four G-type lysozymes, those from ostrich (*13*), black swan (*6*), embden goose (*14*), and cassowary (*15*), and two from the genes of chicken and flounder (*16*, *17*). Recently, Honda and Fukamizo reported the binding mode of GlcNAc oligomer to goose egg-white lysozyme (GEL), and postulated that

*To whom correspondence should be addressed. Tel: +81-9676-7-3918, Fax: +81-9676-7-3960, E-mail: skawa@ktmail.ktokai-u.ac.jp

GEL has six substrate binding subsites (B, C, D, E, F, and G) (*18*). However, only subsites B, C, and D have been directly determined from the crystal structure of a stable complex between GEL and a trimer of *N*-acetylglucosamine, $(GlcNAc)_3$ (*11*). Therefore, clarification of which amino acids are actually involved in substrate binding, especially at subsites E, F, and G, is of particular interest.

In this study, as a first step toward understanding the structure-function relationships of G-type lysozymes, we synthesized chemically the gene coding for ostrich egg-white lysozyme (OEL) based on the published amino acid sequence (*13*) and developed a functional expression system for the mature OEL in yeast *Pichia pastoris*. Furthermore, to obtain essential basic information for future studies involving site-directed mutagenesis, the time-course of the OEL-catalyzed reaction on the substrate $(GlcNAc)_n$ (n = 5 and 6) was measured, and the binding constants of sugar residues at each subsite and the rate constants were estimated from the experimental time-course using the reaction model constructed for GEL (*18*). From these results, the active site properties of OEL were compared with those of GEL.

EXPERIMENTAL PROCEDURES

Materials—Freshly laid ostrich eggs were kindly donated by the Kumamoto Zoological Park (Kumamoto) and Hirakawa Zoological Park (Kagoshima), and OEL was purified from the egg whites by the methods of Jollès *et al*. (*19*) with a slight modification. Six-times recrystallized hen egg-white lysozyme was purchased from Seikagaku Kogyo. *N*-Acetylglucosamine oligosaccharides $[(GlcNAc)_n]$ were prepared by acid hydrolysis of chitin followed by charcoal celite column chromatography (*20*). The BCA protein assay reagent was obtained from Pierce. CM-Toyopearl 650M was obtained from Tosoh. *Micrococcus luteus* cells and Geneticin 418 (G418) were from Sigma. The 32 oligonucleotides with a chain length of 21–48 bases were obtained from Hokkaido System Science. Restriction enzymes and other DNA modifying enzymes were purchased from TaKaRa or Toyobo. The ABI PRIME Dye Terminator Cycle Sequencing Ready Reaction kit was from Perkin-Elmer. All other reagents and chemicals were of analytical grade.

Stains, Plasmids, and Media—E. coli strain JM109 was used for the transformation and propagation of recombinant plasmids. The *P. pastoris* expression system including expression vectors pPIC9 and pPIC9K was purchased from Invitogen. *P. pastoris* GS115 (Invitrogen) was used as the host strain for expression. *E. coli* cells were grown in Luria-Bertani broth. BMGY for growing *P. pastoris*, BMMY for the induction of recombinant proteins, MD plates for transformation, and YPD-G418 plates for the selection of multicopy transformants are described in the Invitrogen manual.

Construction of a Synthetic Gene Encoding OEL—The entire OEL gene was assembled from three parts: the amino terminal part (A), the middle part (B), and the carboxyl terminal part (C) (Figs. 1 and 2). The A part gene was constructed from 9 fully overlapping oligonucleotides ranging in length from 23 to 48 bases (SN1–SN4 and CN1–CN5). The 5′ ends of the oligonucleotides (50 pmol) were phosphorylated by treatment with ATP (5 μM) and T_4 polynucleotide kinase (20 units), except for the two oligos (SN1 and CN5) that were at the extreme 5′ ends of the cassette. After incubation for 1 h at 37°C, the kinase was inactivated by heating at 75°C for 15 min. The phosphorylated fragments and nonphosphorylated ends (2.5 pmol) were mixed in a volume of 10 μl and heated at 95°C for 3 min. The mixture was then cooled slowly to room temperature over 1 h to allow the complementary strands to anneal and treated with T_4 DNA ligase at 16°C for 16 h. The product was ligated into plasmid pBluescript previously digested with *Xho*I and *Hin*dIII. The resulting construct, pBOEL-A, was transformed into *E. coli* strain JM109, and the plasmid was isolated from the transformed cells.

The other two parts were prepared in the same manner as described above, except that the B part gene was constructed by ligating two subfragments (B-I and B-II), as shown in Fig. 2. The entire OEL gene was constructed by stepwise ligation as follows: the B part gene was inserted at the *Hin*dIII and *Sma*I sites of pBOEL-A to yield pBOEL-A/B, and the C part gene was inserted at the *Sma*I and *Not*I sites of pBOEL-A/B to yield pBOEL-A/B/C, which contained the whole gene coding for OEL. At each step and upon completion, the structures of the genes were confirmed by DNA sequence determination with an ABI PRIME 373A DNA Sequencer (Perkin-Elmer Applied Biosystems).

Construction of an Expression Vector and Its Introduction into P. pastoris—The entire gene encoding mature OEL was excised from pBOEL-A/B/C by digestion with *Xho*I and *Not*I, and then ligated into *P. pastoris* vector pPIC9 to yield plasmid pPOEL. This cloning step resulted in the translational fusion of the OEL coding region to that of the *S. cerevisiae* α-factor prepropeptide. Subsequently, the *Bam*HI/*Not*I DNA fragment from pPOEL was recloned into plasmid pPIC9K, resulting in plasmid pPKOEL (Fig. 3), which allows selection of multiple insertions of the expression cassette. The plasmid pPKOEL was digested with *Sal*I and then introduced into *P. pastoris* GS115 (*his*4) by a lithium chloride method according to the manufacturer's instructions (Invitrogen). Recombinant His^+ yeast clones obtained after transformation on MD plates were grown on YPD plates containing Geneticin 418 (0.025–0.05% G418) for selection of multiple insertions (*21*).

Screening for OEL Expression—P. pastoris transformants were cultured in 3 ml of BMGY for 24 h at 30°C. Cells collected from 2 ml of BMGY culture were resuspended in 2 ml of BMMY. The culture was maintained for 3 days with methanol supplementation to a final concentration of 1% every 24 h. The secretion of recombinant OEL (rOEL) into the culture medium was monitored by the lytic activity using the lyophilized cell walls of *Micrococcus luteus* as a substrate, as described previously (*22*).

Overexpression and Purification—A recombinant *P. pastoris* clone harboring the plasmid pPKOEL was typically inoculated into 5 ml of BMGY and incubated at 30°C for 24 h. This seed culture was subcultured into 100 ml of the same medium for an additional 24 h. The cells were harvested and transferred to 900 ml of BMMY to an OD_{600} of 1.0 to induce production. The culture was maintained for

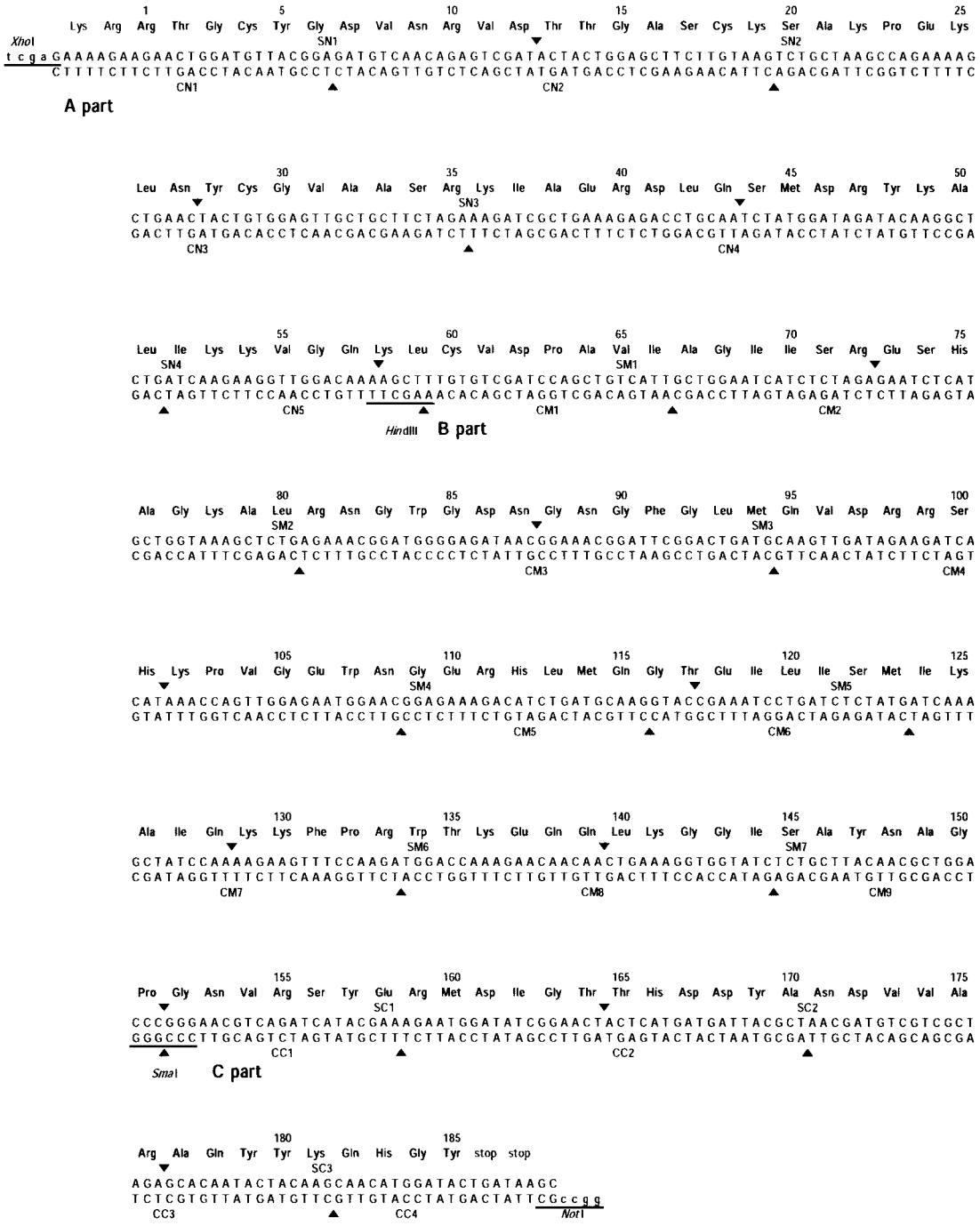

Fig. 1. **The amino acid sequences of OEL and its synthetic gene.** Ligation points are marked by arrowheads. The restriction enzyme recognition sites are underlined.

5 days with methanol supplementation to a final concentration of 1% every 24 h.

The culture was centrifuged for 10 min at 6,000 rpm and the supernatant was brought to pH 8.0 with NaOH. After 5-fold dilution with water, the supernatant was loaded onto a CM-Toyopearl column (1.5 × 12.5 cm) equilibrated with 30 mM sodium phosphate buffer (pH 8.0). After the column was washed, the bound protein was eluted with 0.5 M NaCl in the same buffer. The eluate was diluted 5-fold with water and loaded onto the same column, then eluted with a linear gradient of 0 to 0.4 M NaCl in 30 mM sodium phosphate buffer (pH 7.0). The fraction exhibiting lysozyme activity was further chromatographed on a CM-Toyopearl column (1.0 × 90 cm) equilibrated with 30 mM sodium phosphate buffer (pH 7.0), and the protein was eluted with a linear gradient of 0 to 0.35 M NaCl in the buffer. The homogeneity of the isolated rOEL was confirmed by SDS-PAGE. The purified enzyme was dialyzed against distilled water and lyophilized for storage. The lytic activity was monitored as

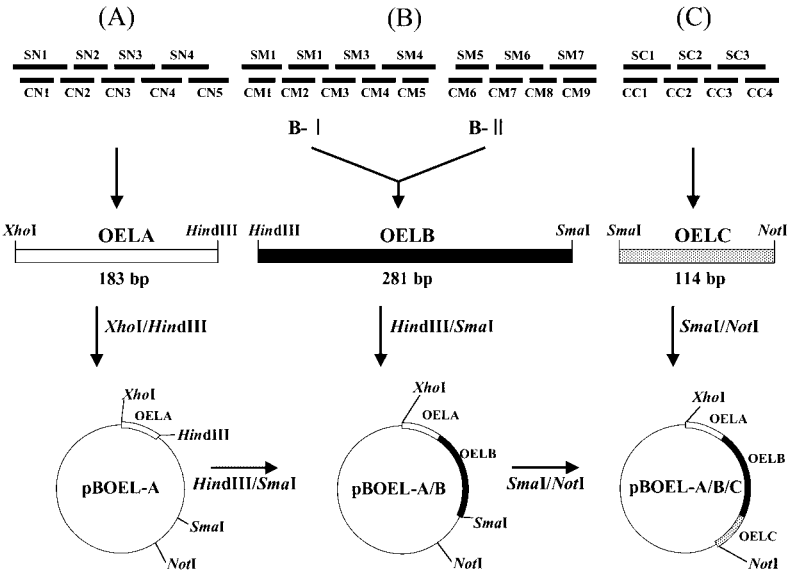

Fig. 2. **Ligation of chemically synthesized oligonucleotides to construct a plasmid (pBOEL-A/B/C) containing a gene coding for full-length OEL.** A total of 32 oligonucleotides were used to assemble the three gene segments (A, B, and C). Separately synthesized gene segments were cloned into the pBluescript vector and ligated to assemble the entire gene. For more details, see "RESULTS AND DISCUSSION."

described previously (*22*). Protein concentrations were determined by the bicinchoninic acid methods (*23*), using hen egg-white lysozyme as a standard protein.

Peptide Mapping—Digestions of reduced and pyridylethylated lysozymes with TPCK-trypsin (Cooper Biomedical, USA) and the separation of the tryptic peptides by reversed-phase high-performance liquid chromatography (RP-HPLC) were accomplished as described previously (*15*). Amino acid analyses were performed on a Hitachi L-8500A amino acid analyzer after hydrolysis of the tryptic peptides with constant boiling HCl containing 0.05% β-mercaptoethanol in evacuated sealed tubes at 110°C for 20 h. The N-terminal sequences of the tryptic peptides were determined on an Applied Biosystems model 477A sequencer.

Circular Dichroism (CD) Spectra—Circular dichroism (CD) spectra were obtained at room temperature with a Jasco J-600 spectropolarimeter. The path-length of the cells was 0.1 cm for far-ultraviolet CD spectra (200–250 nm). Proteins were dissolved to a final concentration of 0.15 mg/ml in 10 mM sodium acetate buffer (pH 5.0). The data were expressed in terms of mean residue ellipticity.

Enzymatic Reaction—The reaction mixture containing 0.1 mM lysozyme and 1 mM $(GlcNAc)_n$ (n = 5 or 6) was incubated in 10 mM sodium acetate buffer (pH 4.0) at 50°C. After a given reaction time, 200 μl of the reaction mixture was withdrawn and rapidly chilled in a KOOL KUP (Towa). The reaction mixture was centrifuged with Ultrafree C3LGC (Millipore), and the filtrate was lyophilized. The dried sample was dissolved in 50 μl of ice-cold water, and then 10 μl of the solution was applied onto a TSK Amide 80 column (4.6 × 250 mm; Tosoh) in a JASCO 800 series HPLC. Elution was performed with 72% acetonitrile at 30°C and a flow rate of 1.0 ml/min. Chitooligosaccharide concentrations were calculated from the peak area monitored by ultraviolet absorption at 220 nm, based on a standard curve obtained with authentic saccharide solutions.

The rate equation of the lysozyme-catalyzed chitooligosaccharide cleavage was solved numerically in order to obtain the calculated time-course by the method reported previously (*18*). In the calculation of the time-course, the rate constant value of k_1 (for the cleavage of the glycosidic linkage) was assumed to be dependent upon the substrate size (*24*). The calculation was repeated with changing values of the rate constants or six binding free energy changes to obtain the calculated time-course with the best fit to the experimental one.

RESULTS AND DISCUSSION

Design and Construction of the Synthetic OEL Gene—In order to investigate the structure-function relationships of G-type lysozyme by means of a genetic engineering approach, it is essential to clone the gene and obtain the recombinant protein in an amount sufficient for structural and biochemical studies in a heterologous expression system. Therefore, we decided to synthesize a gene coding the full-length OEL based on the published amino acid sequence (*13*), since the cDNA sequence of the protein has not yet been reported. Figure 1 shows the amino acid sequence of OEL and its synthetic gene fragments. The structural gene was designed to use yeast *P. pastoris*–preferred codons (*25*), since we intended to express the synthesized gene in *P. pastoris*. The OEL gene was divided into three parts: the amino terminal part (A), the middle part (B), and the carboxyl terminal part (C). Restriction enzyme recognition sites for *Xho*I, *Hin*dIII, *Sma*I, and *Not*I were incorporated to clone the three gene fragments into plasmid pBluescript and to facilitate future work involving site-directed mutagenesis. The entire gene-coding sequence was flanked with the cohesive ends of *Xho*I and *Not*I restriction sites for eventual cloning into the expression vector pPIC9K. The extended N-terminal dipeptide, Lys-Arg, derived from the C-terminus of the α-factor signal sequence was also added at the appropriate position to generate the signal cleavage site.

Figure 2 summarizes the cloning steps involved in constructing the entire OEL gene. The three gene segments (A, B, and C) were constructed by enzymatic ligation of 32 chemically synthesized oligonucleotides ranging in size from 21 to 48 bases. The three gene segments were the

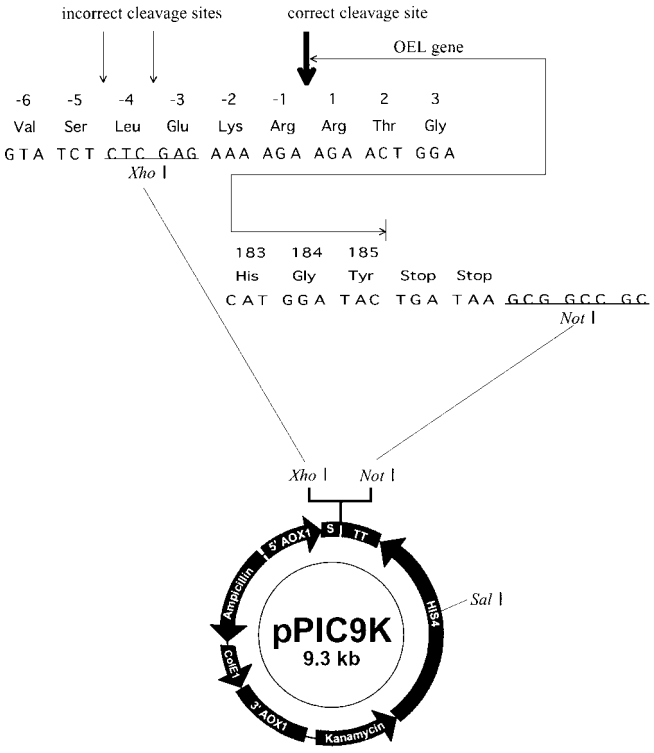

Fig. 3. **Restriction map of the expression vector pPKOEL.** The synthetic OEL gene was inserted between the *Xho*I and *Not*I sites of pPIC9K. The 6 amino acid sequence of the C-terminus of the α-factor signal is shown, as well as part of the mature OEL sequence. The bold and thin arrows in the α-factor signal sequence indicate the positions of correct and incorrect cleavage sites during secretion, respectively.

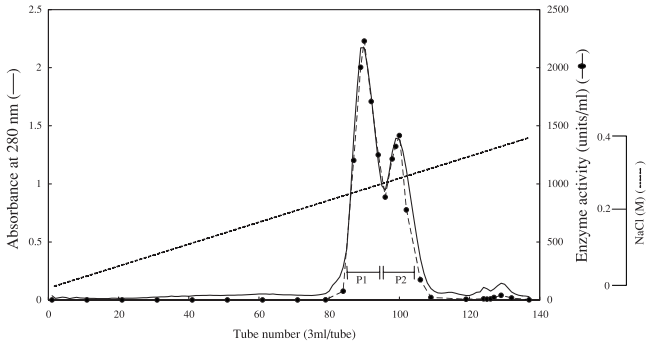

Fig. 4. **Cation-exchange column chromatography for the purification of rOEL.** The culture supernatant was first applied to a CM-Toyopearl column (1.5 × 12.5 cm) equilibrated with 30 mM sodium phosphate buffer (pH 8.0). Fractions containing lysozyme activity were then applied to the same column equilibrated with 30 mM sodium phosphate buffer (pH 7.0). The bound proteins were eluted with a linear gradient of NaCl from 0 to 0.4 M in the same buffer. The lysozyme activity toward *Micrococcus luteus* cells was measured as described in "EXPERIMENTAL PROCEDURES." The active fractions (designated P1 and P2) were pooled as indicated by the horizontal bars.

183 bp *Xho*I/*Hin*dIII fragment (OELA), the 281 bp *Hin*dIII/*Sma*I fragment (OELB), and the 114 bp *Sma*I/*Not*I fragment (OELC). The B-segment was constructed by ligating two subfragments (B-I and B-II). The entire OEL gene (578 bp) was assembled by stepwise ligation of the three gene fragments into pBluescript. The resulting plasmid was named pBOEL-A/B/C. The sequence of the cloned gene was confirmed to be the same as the designed sequence.

Expression and Characterization of Recombinant OEL (rOEL)—The methylotrophic yeast *P. pastoris* has recently attracted attention for its high-level production of proteins, and many kinds of lysozymes have been expressed in this expression system (*26–29*). We therefore attempted to construct the expression system for OEL using yeast *P. pastoris* as an expression host. For this purpose, the synthetic OEL gene excised from pBOEL-A/B/C was fused to the DNA encoding the *S. cerevisiae* α-factor prepropeptide in vector pPIC9K (Fig. 3), the objective being to produce rOEL in the medium. The resulting expression plasmid, pPKOEL, was introduced into His-deficient *P. pastoris* strain GS115 after linearization, and His^+ yeast clones were selected. Recombinant yeast clones carrying plasmid pPKOEL, which contains a kanamycin-resistance gene, were further propagated on G418 plates to select clones with multiple copies of the expression cassette as described previously (*21*). Recombinant *P. pastoris* clones obtained on plates supplemented with 0.05% G418 were cultivated using methanol as an inducer in small volume cultures (2 ml) for 3 days. The clone with the highest level of rOEL secretion was used for overexpression.

The rOEL secreted into the medium was first chromatographed on CM-Toyopearl equilibrated with 30 mM phosphate buffer (pH 8.0), and the bound proteins were eluted with 0.5 M NaCl in the same buffer. The fractions containing lysozyme activity were then applied to the same column equilibrated with 30 mM phosphate buffer (pH 7.0) and eluted with a linear gradient of NaCl. As shown in Fig. 4, two main peaks (P1 and P2) with lysozyme activity were observed, suggesting that the α-factor signal sequence was not digested completely or was digested incorrectly during secretion. The N-terminal amino acid sequences of the secreted proteins were then analyzed for three residues by protein sequencing, and the processing sites (arrows) are shown in Fig. 3. The sequence of fraction P1 was determined to be Arg-Thr-Gly, which coincides with that of authentic OEL, indicating that the protein in P1 corresponds to the lysozyme molecule correctly processed at the C-terminus of the α-factor signal. On the other hand, sequence analysis of fraction P2 gave two N-terminal sequences, Leu-Glu-Lys and Glu-Lys-Arg, both of which exist in the α-factor signal. This result indicates that the products in P2 are a mixture of two molecular species in which three or four additional amino acids of the α-factor signal are attached to the N-terminus of the mature OEL. It was thus found that the α-factor signal sequence was processed at three different positions including the correct site during secretion (Fig. 3). Although we have no appropriate explanation for this phenomenon, the misprocessed sub-products have also been reported when other C-type lysozymes are expressed in yeast expression systems using α-factor as a secretion signal (*29–31*). The correctly processed rOEL (P1 in Fig. 4) was further purified to remove small

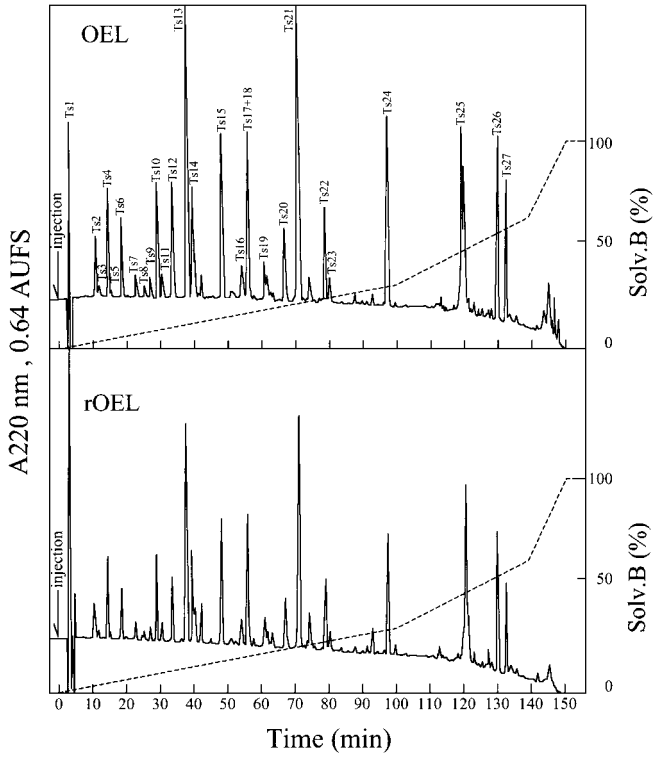

Fig. 5. **Elution profiles of tryptic peptides of authentic OEL and rOEL.** The digested peptides were developed with a gradient elution system of 0.1% TFA (solv. A) and 60% acetonitrile in solv. A (solv. B). A gradient of 0–60% solv. B in 150 min was made. The peptides were detected at 220 nm. Numbers on the peaks are numerical according to the elution order.

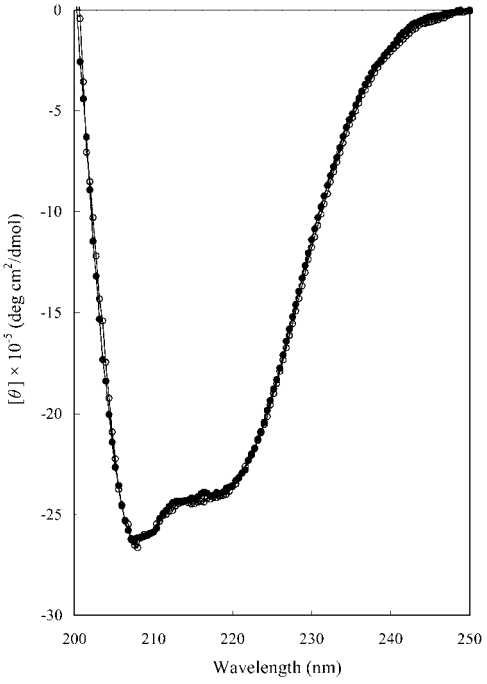

Fig. 6. **CD spectra of authentic OEL and rOEL in the far-ultraviolet region.** Spectra were measured as described in "EXPERIMENTAL PROCEDURES." Closed circles and open circles indicate the CD spectra of authentic OEL and rOEL, respectively.

amounts of contaminants and gave a single band on analysis by SDS-PAGE (data not shown). The yield of rOEL was about 10 mg/liter induced culture.

In order to confirm that the purified rOEL has the correct amino acid sequence, it was reduced, pyridylethylated, digested with TPCK-trypsin, and subjected to peptide mapping on RP-HPLC (Fig. 5). Clearly, all peptides derived from rOEL exhibited the same retention times as those of authentic OEL, indicating that the amino acid sequences of the two lysozymes are identical. The integrity of rOEL was confirmed by measurements of far-ultraviolet CD (200–250 nm) (Fig. 6). The CD spectra of the authentic and recombinant proteins overlapped completely, indicating that there is no detectable difference in their secondary structures. Furthermore, the lytic activity of rOEL against *M. luteus* was found to be the same as that of OEL (data not shown). Therefore, we conclude that the expression system for the production of rOEL with structural and functional properties comparable to those of the authentic form could be established.

Time-Course of GlcNAc Oligosaccharide Digestion by OEL—When investigating lysozyme-catalyzed reactions in detail, it is important to examine the experimental time-course of oligosaccharide digestion, because much information about lysozyme catalysis, such as the splitting mode, subsite structure, and transglycosylation, can then be obtained (*32*). The mode of enzyme action of G-type lysozyme toward GlcNAc oligomer has been investigated only for GEL (*18*). Therefore, the experimental time-course of GlcNAc oligosaccharide digestion by OEL was analyzed to obtain essential basic information for future studies involving site-directed mutagenesis.

The enzymatic hydrolysis of $(GlcNAc)_6$ by rOEL is shown in Fig. 7A. The time-course for rOEL was found to be indistinguishable from that for authentic OEL, further confirming that the rOEL produced by yeast was correctly folded into an active conformation practically the same as that of OEL (data not shown). Under the experimental conditions used, the initial substrate $(GlcNAc)_6$ disappeared almost completely after 50 min of reaction. From $(GlcNAc)_6$, OEL produced abundant amounts of $(GlcNAc)_3$ and lesser amounts of $(GlcNAc)_2$ and $(GlcNAc)_4$, while $(GlcNAc)_1$ and $(GlcNAc)_5$ were produced in much smaller amounts. The product $(GlcNAc)_5$ was immediately hydrolyzed further to $(GlcNAc)_2$ + $(GlcNAc)_3$ and $(GlcNAc)_1$ + $(GlcNAc)_4$. Product distribution was $(GlcNAc)_3 \gg (GlcNAc)_2 > (GlcNAc)_4 > (GlcNAc)_1 > (GlcNAc)_5$. This indicates that OEL hydrolyzes the substrate in an endo-splitting manner. Considering the fact that two molecules of $(GlcNAc)_3$ are produced from $(GlcNAc)_6$, the frequency of cleavage to $(GlcNAc)_3$ + $(GlcNAc)_3$ appears to be considerably higher than that of cleavage to $(GlcNAc)_2$ + $(GlcNAc)_4$. Thus, OEL appears to hydrolyze preferentially the third glycosidic linkage from the nonreducing end of $(GlcNAc)_6$. Oligosaccharide products with a degree of polymerization higher than that of the initial substrate were not observed, indicating that OEL does not catalyze transglycosylation. The substrate $(GlcNAc)_5$ was then digested by OEL and the time-course

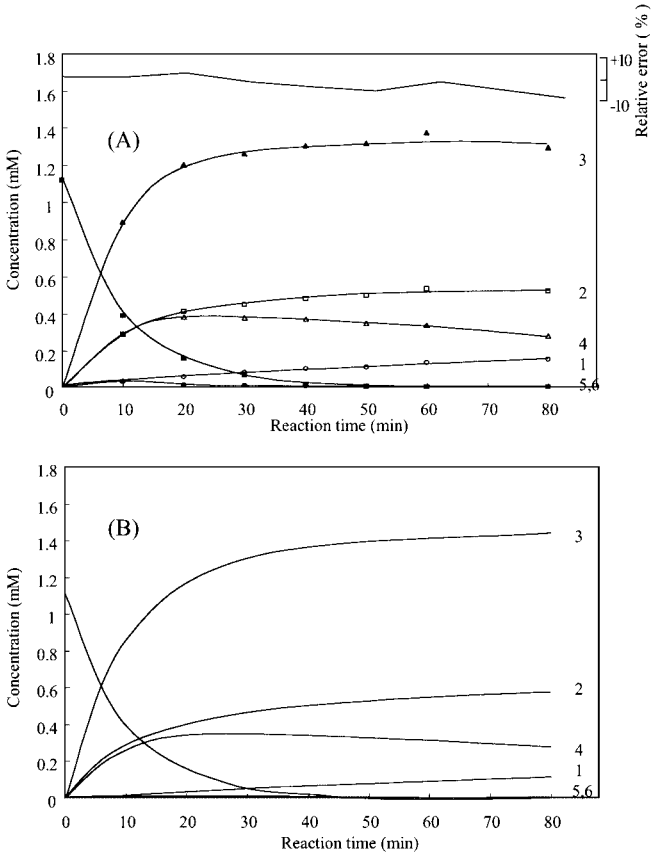

Fig. 7. **Time-course of $(GlcNAc)_6$ degradation by rOEL.** Panel A shows the experimental time-course of rOEL. The initial concentrations of enzyme and substrate were 0.1 and 1 mM, respectively. The solid lines were drawn by roughly following the experimental data points. Panel B shows the calculated time-course of rOEL. The parameter values used for the calculation are listed in Table 1. Numbers in the figures represent the polymerization degrees of the reaction products.

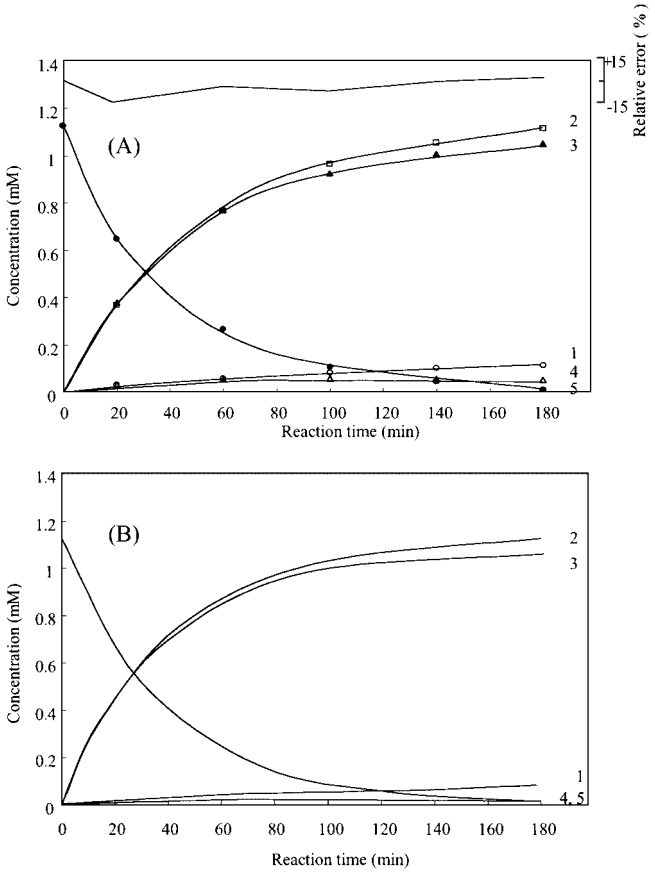

Fig. 8. **Time-course of $(GlcNAc)_5$ degradation by rOEL.** Panel A shows the experimental time-course of the degradation of $(GlcNAc)_5$ by rOEL. The reaction conditions were the same as in Fig. 7. The solid lines were drawn by roughly following the experimental data points. Panel B shows the calculated time-course for rOEL. The parameter values used for the calculation are listed in Table 1. Numerals indicate the polymerization degrees of the reaction products.

was obtained under the same conditions (Fig. 8A). OEL also hydrolyzed $(GlcNAc)_5$ in an endo-splitting manner, although the reaction rate was lower than that of $(GlcNAc)_6$ hydrolysis. $(GlcNAc)_5$ was hydrolyzed mainly to $(GlcNAc)_2$ + $(GlcNAc)_3$ with much less cleavage to $(GlcNAc)_1$ + $(GlcNAc)_4$.

Since the product distribution produced by OEL was similar to that seen for GEL (*18*), these two lysozymes are believed to share the same type of subsite structure. However, the profile of the time-course of $(GlcNAc)_6$ degradation for OEL differed slightly from that for GEL: in the case of OEL, the generated $(GlcNAc)_4$ decomposed gradually, accompanied by a slight increase in the amounts of $(GlcNAc)_1$, $(GlcNAc)_2$, and $(GlcNAc)_3$ (Fig. 7A). The product $(GlcNAc)_4$ would be hydrolyzed to $(GlcNAc)_2$ + $(GlcNAc)_2$ or $(GlcNAc)_1$ + $(GlcNAc)_3$, and the products $(GlcNAc)_2$ and $(GlcNAc)_3$ would not be further hydrolyzed. The product $(GlcNAc)_4$ also decomposed slowly over the time-course of $(GlcNAc)_5$ hydrolysis (Fig. 8A). However, this decomposition of the intermediate product $(GlcNAc)_4$ was not observed in the time-course of GEL (*18*), suggesting that the binding mode of the oligosaccharide to OEL is globally similar to that to GEL, but somewhat different in some details.

Theoretical Analysis of the Experimental Time-Course—Subsequently, the experimental time-course of $(GlcNAc)_6$ degradation was analyzed by computer simulation in order to obtain the rate constants and the binding free energy values of the individual subsites. The theoretical model used for the analysis of GEL (*18*), in which six binding subsites (B, C, D, E, F, and G) and bond cleavage between subsites D and E are postulated, was employed in the analysis of the OEL-catalyzed reaction. The calculated time-course of OEL is shown in Fig. 7B and the reaction parameters obtained are summarized in Table 1 together with the values for GEL. We obtained optimized free energy values of –0.3, –2.2, +4.2, –2.0, –2.6, and –2.5 kcal/mol for the corresponding subsites of OEL. The rate constant k_2 for hydration was set at the value estimated for GEL (*18*), 100.0 s^{-1}. The rate constants k_1 for the cleavage of the glycosidic linkage were estimated to be 1.20 s^{-1} for $(GlcNAc)_4$, 0.20 s^{-1} for $(GlcNAc)_5$, and 0.35 s^{-1} for $(GlcNAc)_6$. Since the calculated time-course closely reflected the amounts of $(GlcNAc)_4$ and $(GlcNAc)_6$ in the

Table 1. **Estimated reaction parameter values for OEL and GEL.**

		Rate constants (s^{-1})		Binding free energy (kcal/mol)					
		k_1	k_2	B	C	D	E	F	G
OEL	$(GlcNAc)_6$	0.35							
	$(GlcNAc)_5$	0.20	100.0	–0.3	–2.2	4.2	–2.0	–2.6	–2.5
	$(GlcNAc)_4$	1.20							
GEL[a]	$(GlcNAc)_6$	0.015							
	$(GlcNAc)_5$	0.006	100.0	–0.5	–2.2	4.2	–1.5	–2.6	–2.8
	$(GlcNAc)_4$	0.003							

[a]From Ref. *18*. k_1 and k_2 are the rate constants of cleavage of the glycosidic linkage and hydration, respectively.

reaction time-course, the k_1 values obtained for $(GlcNAc)_4$ and $(GlcNAc)_6$ were considered to be optimal for the OEL-catalyzed reaction. However, it was difficult to estimate precisely the k_1 value for $(GlcNAc)_5$ because the amount of $(GlcNAc)_5$ produced was very small during the reaction time-course. To confirm further the validity of the parameter values obtained, we tried to calculate the time-course of $(GlcNAc)_5$ degradation using the same values listed in Table 1. As shown in Fig. 8A, the profile of the theoretical time-course was in good agreement with that obtained experimentally. Therefore, we conclude that the kinetic parameters estimated from $(GlcNAc)_6$ hydrolysis are most appropriate for the OEL-catalyzed reaction.

Although the subsite structure of OEL was estimated to be identical to that of GEL, the binding free energy values for subsites B and G for OEL were decreased by 0.2 and 0.3 kcal/mol, respectively, compared with those of GEL (Table 1). Furthermore, the binding free energy value for site E for OEL was found to be –2.0 kcal/mol, which is –0.5 kcal/mol higher than that of GEL. These data indicate that the substrate binding for OEL is different from that for GEL at or near subsites B, E, and G, and that the characteristic time-course of OEL may be due to the change in the affinities of the substrate for these sites from those of GEL. The rate constant value k_1, which reflects the catalytic potency of the glutamic acid residue (Glu73) at the catalytic site, also differed significantly between the two lysozyme: the k_1 value for OEL was much larger than that for GEL. However, a reasonable explanation for this point cannot be given at present because of the differences in the experimental conditions used.

OEL shares 84% amino acid identity with GEL, and the substrate-binding residues proposed for GEL (*11*) are mostly conserved in OEL, the exceptions being those corresponding to Asn122 and Phe123 of GEL, which are located at subsite B. Asn122 and Phe123 in GEL are replaced by Ser and Met in OEL, respectively. Since the binding free energy values at subsite B are different between OEL and GEL (Table 1), the different cleavage profiles of the two lysozymes may be partly explained by these two substitutions. The free energy differences at subsites E and G may also contribute to the different cleavage profiles. However, further discussion on this point is impossible at the present time, since information about subsites E, F, and G is quite limited. Thus, further studies are required to define the different kinetic properties of OEL and GEL.

In this investigation, we show that rOEL can be produced using the yeast *P. pastoris* expression system and purified by a three-step chromatographic procedure. The rOEL thus obtained had the same properties as the authentic protein with respect to activity-measurement and far-UV CD spectrum. To our knowledge, this is the first report in which a high-level expression system for a G-type lysozyme has been achieved, and it is hoped that this will allow further structural and functional investigations by means of site-directed mutagenesis.

We wish to thank Kumamoto Zoological Park (Kumamoto) and Hirakawa Zoological Park (Kagoshima) for supplying the eggs.

REFERENCES

1. Canfield, R.E. (1963) The amino acid sequence of egg white lysozyme. *J. Biol. Chem.* **238**, 2698–2707
2. Jollès, J., Jauregui-Adell, J., Bernier, I., and Jollès, P. (1963) La structure chimique du lysozyme de blanc d'oeuf de poule: etude detailee. *Biochim. Biophys Acta* **78**, 668–689
3. Blake, C.C.F., Koenig, D.F., Mair, G.A., North, A.C.T., Phillips, D.C., and Serma, V.R. (1965) Structure of hen egg white lysozyme. A three-dimensional Fourier synthesis at 2 Å resolution. *Nature* **206**, 757–761
4. Inoue, M., Imada, M., and Tsugita, A. (1970) The amino acid sequence of T4 phage lysozyme. IV. Diluted acid hydrolysis and order of tryptic peptides. *J. Biol. Chem.* **245**, 3479–3484
5. Matthews, B.W. and Remington, S.J. (1974) The three-dimensional structure of the lysozyme from bacteriophage T4. *Proc. Natl. Acad. Sci. USA* **71**, 4178–4182
6. Simpson, R.J. and Morgan, F.J. (1983) Complete amino acid sequence of embden goose (*Anwer anwer*) egg-white lysozyme. *Biochim. Biophys Acta* **744**, 349–351
7. Grütter, M.G., Weaver, L.H., and Matthews, B.W. (1983) Goose lysozyme structure: an evolutionary link between hen and bacteriophage lysozyme? *Nature* **303**, 828–831
8. Isaacs, N.W., Machin, K.J., and Masakuni, M. (1985) Three-dimensional structure of goose-type lysozyme from the egg white of the Australian black swan, Cygnus atratus. *Aust. J. Biol. Sci.* **38**, 13–22
9. Weaver, L.H., Grütter, M.G., Remington, S.J., Gray, T.M., Isaacs, N.W., and Matthews, B.W. (1985) Comparison of goose-type, chicken-type, and phage-type lysozymes illustrates the changes that occur in both amino acid sequence and three-dimensional structure during evolution. *J. Mol. Evol.* **21**, 97–111
10. Anderson, W.F., Grütter, M.G., Remington, S.J., and Matthews, B.W. (1981) Crystallographic determination of the mode of binding of oligosaccharide to T4 bacteriophage lysozyme: implications for the mechanism of catalysis. *J. Mol. Biol.* **147**, 523–543

11. Weaver, L.H., Grütter, M.G., and Matthews, B.W. (1995) The refined structures of goose lysozyme and its complex with trisaccharide show that the "goose type" lysozyme lack a catalytic aspartate residue. *J. Mol. Biol.* **245**, 54–68
12. Arnheim, N., Inouye, M., Law, L., and Laudin., A. (1973) Chemical studies on the enzymatic specificity of goose egg white lysozyme. *J. Biol. Chem.* **248**, 233–236
13. Schoentgen, F., Jollès, J., and Jollès, P. (1982) Complete amino acid sequence of Ostrich (*Struthio camelus*) egg white lysozyme, a goose type lysozyme. *Eur. J. Biochem.* **123**, 489–497
14. Simpson, R.J. and Morgan, F.J. (1982) Complete amino acid sequence of embden goose (*Anwer anwer*) egg white lysozyme. *Biochim. Biophys Acta* **744**, 489–497
15. Thammasirirak, S., Torikata, T., Takami, K., Murata, K., and Araki, T. (2002) The primary structure of Cassowary (*Casuarius casuarius*) goose type lysozyme. *Biosci. Biotechnol. Biochem.* **66**, 147–156
16. Nakano, T. and Graf, T. (1991) Goose type lysozyme gene of the chicken: Sequence genomic organization and expression reveals major differences to chicken-type lysozyme gene. *Biochim. Biophys Acta* **1090**, 273–276
17. Hikima, J., Minagawa, S., Hirono, I., and Aoki, T. (2001) Molecular cloning, expression and evolution of the Japanese flounder goose-type lysozyme gene, and the lytic activity of its recombinant protein. *Biochim. Biophys Acta* **1520**, 35–44
18. Honda, Y. and Fukamizo, T. (1998) Substrate binding subsites of chitinase from barley seeds and lysozyme from goose egg white. *Biochim. Biophys Acta* **1388**, 53–65
19. Jollès, J., Perin, J.P., and Jollès, P. (1977) The ostrich (*Struthio camelus*) egg white lysozyme. *Mol. Cell. Biochem.* **17**, 39–44
20. Rupley, J.A. (1964) The hydrolysis of chitin by concentrated hydrochloric acid, and the preparation of low-molecular weight substrates for lysozyme. *Biochim. Biophys Acta* **83**, 245–255
21. Weiss, H.M., Hasse, W., Michel, H., and Reilander, H. (1998) Comparative biochemical and pharmacological characterization of the mouse $5HT_{5A}$ 5-hydroxytryptamine receptor and the human β_2-adrenergic receptor produced in the methylotrophic yeast *Pichia pastoris*. *Biochem. J.* **330**, 1137–1147
22. Thammasirirak, S., Torikata, T., Takami, K., Murata, K., and Araki, T. (2001) Purification and characterization of goose type lysozyme from Cassowary (*Casuarius casuarius*) egg white. *Biosci. Biotechnol. Biochem.* **65**, 584–592
23. Smith, P.K., Krohn, R.I., Hermanson, G.T., Mallia, A.K., Garther, F.H., Provenzano, M.D., Fujimoto, E.K., Goeke, N.M., Olson, B.J., and Klenk, D.C. (1985) Measurement of protein using bicinchroninic acid. *Anal. Biochem.* **150**, 76–85
24. Fukamizo, T., Minematsu, T., Yanase, Y., Hayashi, K., and Goto, S. (1986) Substrate size dependence of lysozyme-catalyzed reaction. *Arch. Biochem. Biophys*. **250**, 312–321
25. Sharp, P.M., Cowe, E., Higgins, D.G., Shields, D.C., Wolfe, K.H., and Wright, F. (1988) Codon usage patterns in *Escherichia coli*, *Bacillus subtilis*, *Saccharomyces cerevisiae*, *Schizosaccharomyces pombe*, *Drosophila melanogaster*, and *Homosapiens*: A review of the considerable within-species diversity. *Nucleic Acids Res.* **16**, 8207–8211
26. Brierley, R.A., Bussineau, C., Kooson, R., Melson, A., and Siegel, R.S. (1990) Fermentation development of recombinant *Pichia pastoris* expressing the heterologous gene: bovine lysozyme. *Ann. N. Y. Acad. Sci.* **589**, 350–362
27. Mine, S., Ueda, T., Hashimoto, Y., Tanaka, Y., and Imoto, T. (1999) High-level expression of uniformly ^{15}N-labeled hen lysozyme in *Pichia pastoris* and identification of the site in hen lysozyme where phosphate ion binds using NMR measurements. *FEBS Lett.* **448**, 33–37
28. Goda, S., Takano, K., Yamagata, Y., Katakura, Y., and Yutani, K. (2000) Effect of extra N-terminal residues on the stability and folding of human lysozyme expressed in *Pichia pastoris*. *Protein Eng.* **13**, 299–307
29. Koganesawa, N., Aizawa, T., Masaki, K., Matsuura, A., Nimori, T., Bando, H., Kawano, K., and Nitta, K. (2001) Construction of an expression system of insect lysozyme lacking thermal stability: the effect of secretion of signal sequence on level of expression in the *Pichia pastoris* expression system. *Protein Eng.* **14**, 705–710
30. Hashimoto, Y., Koyabu, N., and Imoto, T. (1998) Effects of signal sequences on the secretion of hen lysozyme by yeast: construction of four secretion cassette vectors. *Protein Eng.* **11**, 75–77
31. Hashimoto, Y., Koyabu, N., and Imoto, T. (1998) Optimization of cultivation time for recombinant protein expression from yeast using αF signal sequence. *Protein Pept. Lett.* **5**, 15–18
32. Masaki, A., Fukamizo, T., Otakara, A., Torikata, T., Hayashi, K., and Imoto, T. (1981) Lysozyme-catalyzed reaction of chitooligosaccharides. *J. Biochem.* **90**, 527–533